Macromolecules
ARTICLE

Macromolecules **2010**, *43*, 3911–3915 **3911**
DOI: 10.1021/ma1002744

Toughening of Nylon-6 by Semicrystalline Poly(vinylidene fluoride): Role of Phase Transformation and Fibrillation of Dispersed Particles

Bing Na,* Wenfei Xu, Ruihua Lv, Zhujun Li, Nana Tian, and Shufen Zou

Department of Materials Science and Engineering, East China Institute of Technology, Fuzhou, 344000, People's Republic of China

Received February 4, 2010; Revised Manuscript Received March 16, 2010

ABSTRACT: Superior toughness has been achieved in the nylon-6/PVDF blends with semicrystalline PVDF component as the dispersed particles. Morphological observations on the impact tested specimens unambiguously reveal the formation of voids and microfibrils across the fracture surface, suggesting that some extent of plastic deformation occurs within ductile PVDF particles. It is further confirmed by the structural evolution at crack tips through micro-FTIR studies on the quasi-static stretching of precracked films. During fracture $\alpha \rightarrow \beta$ phase transformation of dispersed PVDF particles first takes place, followed by the extensive plastic deformation and fibrillation of new-formed β-crystals. It is believed that the $\alpha \rightarrow \beta$ phase transformation and fibrillation of β-crystals of the dispersed PVDF particles are responsible for the toughness enhancement in the nylon-6/PVDF blends with good interfacial adhesion.

1. Introduction

Like most semicrystalline polymers, nylon-6 behaves brittle in the presence of cracklike flaws and notches.[1] One conventional and effective routine for toughening is to incorporate some amount of soft rubber particles in the nylon-6 matrix.[2−5] The presence of soft particles can induce extensive plastic flow of nylon-6 matrix among them once the critical interparticle ligament thickness is achieved[2,6−8] and thus is beneficial for the significant energy absorption during fracture. In addition, rubber particles cavitation is also contributed to the improved toughness as a result of the release of triaxial tensile stress.[2,3,9] However, the loss of stiffness and strength, in parallel with toughness enhancement, also becomes obvious in the rubber-modified nylon-6.

Alternatively, blending of nylon-6 with inorganic or organic rigid particles to improve its toughness is another pursuit in the polymer community. As a matter of fact, the toughness of nylon-6 can only be increased to some extent[10] or becomes deteriorated[11] with incorporation of inorganic particles because of high plastic resistance and incomplete debonding of inorganic particles from the matrix. On the other hand, amorphous polymers, including acrylonitrile-*co*-styrene (AS), polysulfone (PSU), and so on, are able to toughen nylon-6, provided that the good interfacial adhesion between the dispersed particles and nylon-6 matrix is guaranteed.[12,13] Moreover, the underlying toughening mechanism is totally different from that prevailed in the rubber-modified polymers. The concept of cold drawing, proposed by Kurauchi et al. on the studies of polycarbonate (PC)/acrylonitrile−styrene copolymer (AS) system,[14] seems be pertinent to the toughening mechanism of rigid organic particles toughened polymers. It is believed that that the plastic deformation of brittle particles in the matrix, instead of shear yielding of the matrix induced by the organic particles, is responsible for the enhanced energy absorption.

In addition, incorporation of semicrystalline poly(vinylidene fluoride) (PVDF) particles in the nylon-6 matrix can also impart toughening effect,[15,16] analogous to that observed in the system modified by rigid amorphous polymers. Generally, the toughness enhancement is resulted from the fine dispersed PVDF domains and in particular good interfacial adhesion between two phases. To date, the toughening mechanism in the nylon-6/PVDF blends still remains mysterious, even though it has been claimed that there is no possible analogy between nylon-6/PVDF blends and rubber-modified polymers.[15]

In this study the toughening mechanism in the nylon-6/PVDF blends with PVDF component as the dispersed particles has been clarified through morphological observations and in particular the structural evolution at crack tips by micro-FTIR measurements. It is indicated that the $\alpha \rightarrow \beta$ phase transformation and fibrillation of newly formed β-crystals within the dispersed PVDF particles during fracture is the origin of enhanced toughness.

2. Experimental Section

2.1. Materials and Sample Preparation. Nylon-6 with intrinsic viscosity of 1.4 dL/g and poly(vinylidene fluoride) with MFI of 15 g/10 min were obtained from BASF and Changshu Fluorine ST Co., China, respectively. Prior to processing, both materials were dried in a vacuum oven at 80 °C overnight. Nylon-6/PVDF blends with desired compositions were melt-blended in an internal mixer at 240 °C for 10 min. Plates with thickness of 0.5 mm and rectangle bars (4 mm thickness × 10 mm width) were prepared by compression molding and injection molding at 240 °C, respectively.

2.2. Mechanical Tests. Tensile deformation of a dog-bone specimen (4 mm width × 6 mm gauge length), punched from the 0.5 mm thick plates, was performed at room temperature using an universal testing machine with a crosshead speed of 2 mm/min. Izod impact measurements on the rectangle bars with a standard notch were carried out by an Izod tester at room temperature.

2.3. Structural Characterizations. *SEM*. Morphological observations were conducted on a Hitachi S3400 SEM instrument. To evaluate the phase morphology, the samples were first cryofractured in liquid nitrogen, followed by etching in dimethyl sulfoxide (DMSO) at 80 °C for 6 h to remove the PVDF phase. To observe the fracture morphology, the specimens collected after Izod impact tests were directly used.

*Corresponding author: Fax 0086-794-8258320; e-mail bingnash@163.com, bna@ecit.edu.cn.

Published on Web 03/26/2010

DSC. The thermal behaviors were registered using a NETZSCH DSC 204 at a rate of 10 °C/min. Melting traces were recorded by heating the samples up to 240 °C, and the crystallization thermograms were subsequently obtained by cooling the samples after being held at 240 °C for 5 min to erase any possible thermal history.

XRD. The crystalline phase was determined by an X-ray diffractometer, and the wavelength of the monochromated X-ray was 0.154 nm.

2.4. Micro-FTIR Measurements. The structural evolution at crack tips during stepwise stretching of a precracked specimen at 2 mm/min was monitored by a Thermo Nicolet infrared microscope with a MCT detector coupled with a ministretcher at room temperature. An adjustable aperture was used to obtain desired microsampling area, e.g., $20 \times 20\ \mu m^2$ in this case. After stretched to a certain elongation, the transmitted IR light was precisely irradiated on the sampling region ahead of crack tips at loading state by moving the sample stage under a CCD view system of the IR microscope. Polarized infrared spectra (by rotating a ZnSe polarizer), parallel and perpendicular to the stretching direction, were collected with a resolution of 4 cm^{-1}, and a total of 64 scans were added for a better signal/noise ratio.

3. Results and Discussion

3.1. Phase Morphology and Crystallization Behaviors. Figure 1 shows the phase morphology of nylon-6/PVDF blends with a composition of 70/30 and 50/50. Note that the PVDF domains manifest themselves as the holes in the images due to etching by DMSO. In both compositions a sea−island structure is observed, where the submicrometer PVDF particles are dispersed in the continuous nylon-6 matrix. The formation of fine dispersed particles is mainly originated from the low interfacial tension,[17] which in turn suggests good interfacial adhesion between the dispersed PVDF phase and nylon-6 matrix. Actually, through lap shear strength measurements it has been well demonstrated that the interfacial adhesion in the nylon-6/PVDF blends is notable due to favorable mutual interactions between them,[15] as compared with other polymer pairs such as polypropylene/nylon-6 with large domain size. Note that the increased domain size of PVDF component with its content in the blends is ascribed to the significant droplet coalescence during melt mixing.[18]

Furthermore, the fine domain size of PVDF component is verified by its retarded crystallization habits, as shown in Figure 2. The crystallization temperature of PVDF component in the blends becomes much lower than that recorded from its pure counterpart, and the smaller domain size, the lower crystallization temperature is. This domain size dependence of crystallization, namely confined crystallization, is a common observation in the microphase-separated block copolymers[19,20] and immiscible polymer blends with fine domain size.[21] It is deemed that homogeneous nucleation is responsible for the confined crystallization since the available heterogeneous nuclei in each domain are reduced significantly with decreasing of domain size. In parallel with retarded crystallization temperature, correspondingly, the melting temperature of PVDF component in the blends decreases to some extent. Even so, the confined crystallization in the small domains has almost no impact on the crystal modification of PVDF component. As demonstrated by the XRD profiles in Figure 3, α-crystals of PVDF phase prevail in the blends, the same as that observed in its pure counterpart.

3.2. Toughness and Fracture Morphology. Figure 4 presents the mechanical properties of nylon-6/PVDF blends

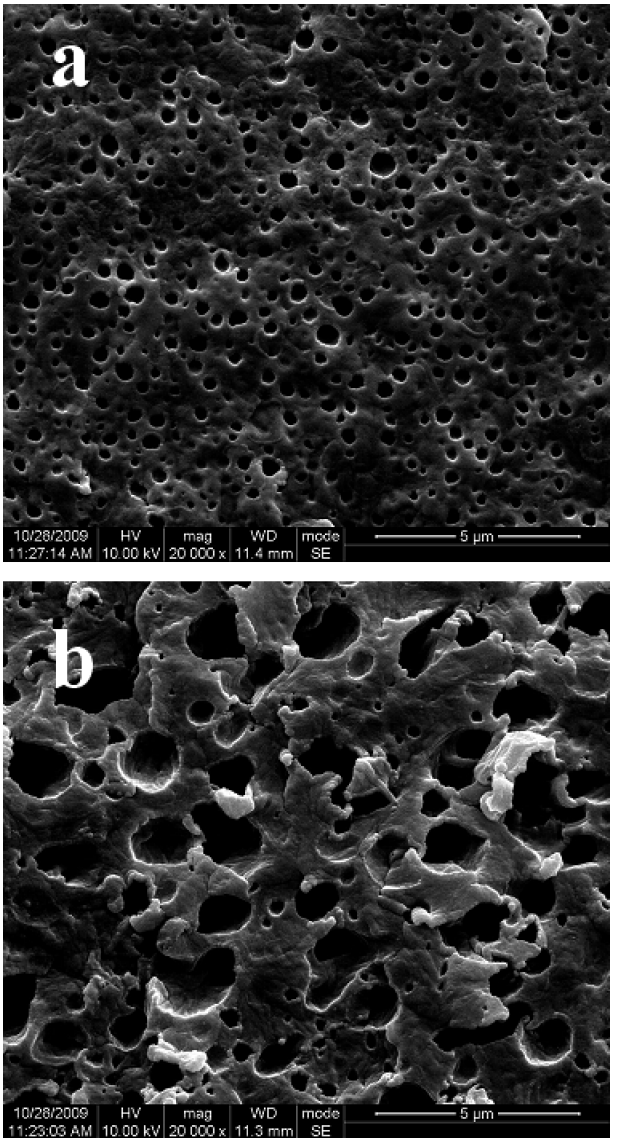

Figure 1. Phase morphology of nylon-6/PVDF blends with different compositions by weight: (a) 70/30, (b) 50/50. Note that in both images the dispersed PVDF particles are represented by the holes due to etching by DMSO.

with PVDF components as the dispersed phase. For comparison, the ones obtained from the pure nylon-6 and PVDF are also included. In line with other observations,[15] superior impact strength is achieved in the blends and becomes significant with increasing PVDF content. Rather, incorporation of the dispersed PVDF particles in the nylon-6 matrix reduces the modulus and yield strength to some extent, analogous to that observed in the rubber modified nylon-6. In common sense, the enhanced toughness in the nylon-6/PVDF blends could be resulted from the small domain size of the dispersed PVDF phase and good interfacial adhesion between two phases. Even so, the detailed toughening mechanism by the semicrystalline PVDF particles still remains unclear.

To clarify it, morphological features of the impact fractured surfaces are checked, and the corresponding results are collected in Figure 5. At a glance, it appears almost no difference between pure nylon-6 and its blends with PVDF component, and only relative flat fracture surface is observed. It means that the dispersed particles activated shear yielding of nylon-6 matrix scarcely occurs in

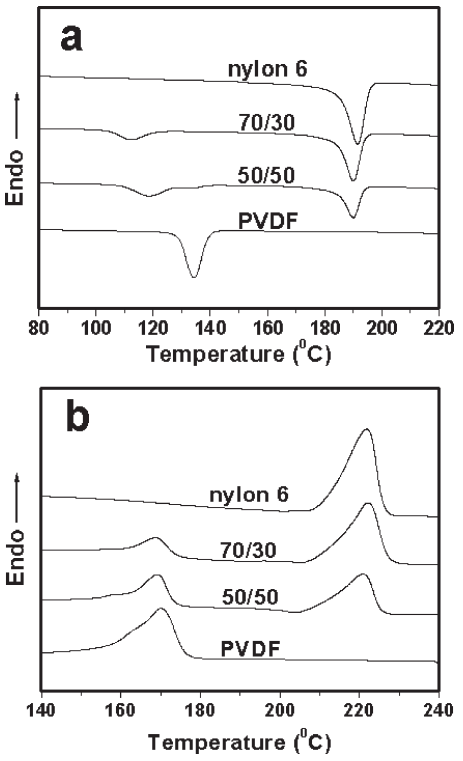

Figure 2. Crytallizaiton (a) and melting traces (b) obtained from nylon-6/PVDF blends with indicated compositions. For comparison, the ones obtained from the pure nylon-6 and PVDF are also included.

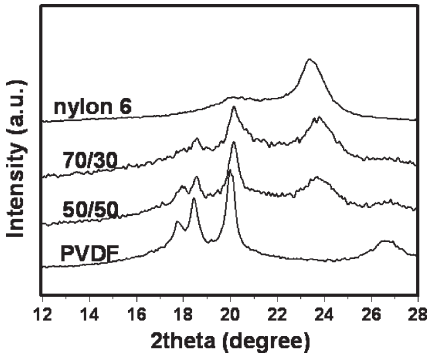

Figure 3. XRD profiles of nylon-6/PVDF blends with indicated compositions. For comparison, the ones obtained from the pure nylon-6 and PVDF are also included. Note that only α-form is observed for both nylon-6 and PVDF components, irrespective of compositions.

the toughened nylon-6/PVDF blends, though the surface-to-surface interparticle distance in these blends roughly meets the requirements of critical ligament thickness (0.3−0.5 μm) for toughening nylon-6 with high plastic resistance.[2] Indeed, for the rubber-modified nylon-6 significant shear yielding of matrix can enhance the toughness by tens of times, accompanied by formation of very rough fracture surface due to enhanced crack propagation resistance, while the critical ligament thickness among soft particles is satisfied.[2,5,22] Nevertheless, it is not a fact in this case (see Figures 4 and 5), and thus the toughening mechanism prevailed in the rubber-modified polymers could be discarded.

Interestingly, a close inspection reveals the presence of voids and elongated microfibrils across the fracture surface in the nylon-6/PVDF blends (see an example shown in Figure 5d), which is absent in the pure nylon-6. The

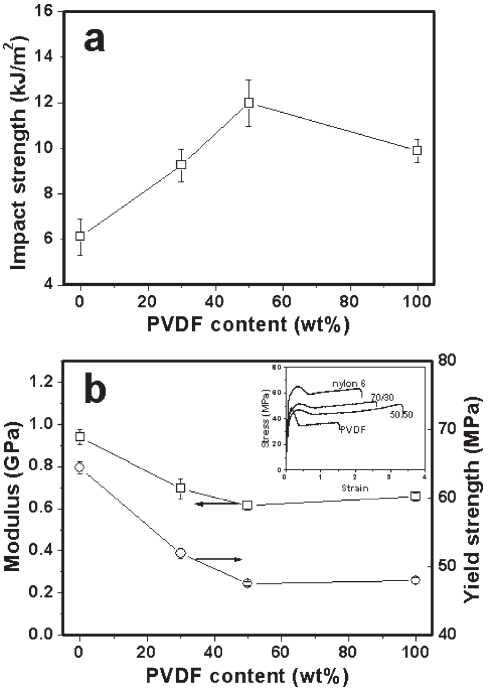

Figure 4. Composition-dependent impact strength (a) and modulus and yield strength (b) in the nylon-6/PVDF blends. Note that the stress−strain curves obtained from tensile tests are included in (b) as an inset.

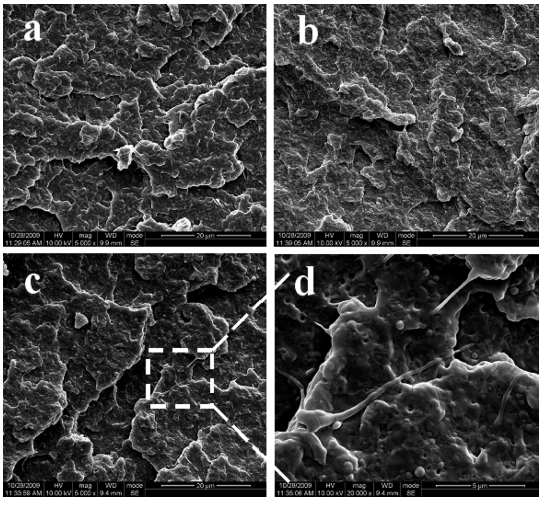

Figure 5. SEM photographs revealing the fracture morphology of pure nylon-6 (a) and nylon-6/PVDF blends (b: 70/30; c, d: 50/50).

formation of voids and microfibrils corresponds to the pull-out and fibrillation of dispersed PVDF particles during impact tests, respectively. Thus, it is expected that some extent of plastic deformation occurs within ductile PVDF particles even pulled out from the matrix due to good interfacial adhesion in the nylon-6/PVDF blends, which is essentially different from the debonding of rigid inorganic filler in the CaCO3/nylon-6 blends with negligible interfacial adhesion.[10] Of course, fibrillation is the extreme example of plastic deformation of dispersed PVDF particles. This argument is somewhat consistent with the cold drawing concept presented in the brittle organic particles toughened ductile polymers,[12−14] although the PVDF component itself is ductile in nature. Hence, the pull-out and fibrillation of dispersed PVDF particles, accompanied

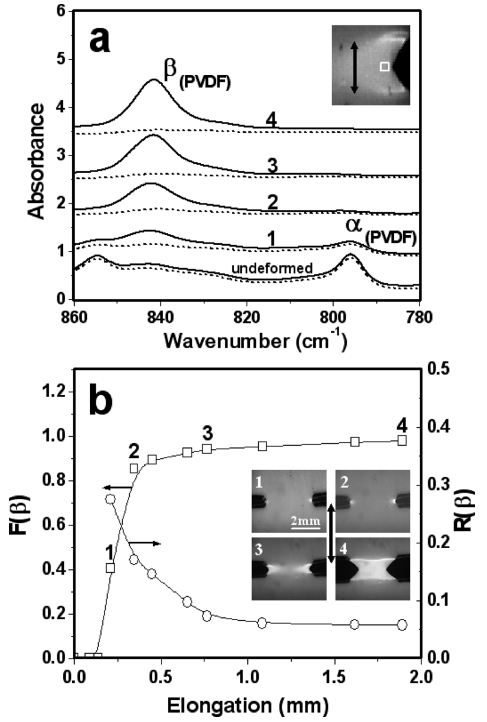

Figure 6. (a) Polarized IR spectra, parallel (dashed lines) and perpendicular (solid lines) to the stretching direction, and (b) relative content $F(\beta)$ and dichroic ratio $R(\beta)$ of the β-form of PVDF component obtained from a small region ahead of crack tips during stretching precracked film of nylon-6/PVDF = 50/50 blends. The simultaneous images recorded during the fracture process are included in (b) as an inset. Note that in (a) the white square on the image represents the sampling position during IR measurements schematically, and the vertical shift of the IR spectra has been done for clarification.

by crack deflection,[10] could dissipate energy to a large extent and result in the toughness enhancement. One may argue that it is not totally convincing only judged from the morphological observations, and detailed information about the plastic deformation of PVDF particles embedded in the nylon-6 matrix during fracture is required. However, it is nearly impossible to obtain the structural evolution during crack initiation and propagation under Izod impact tests with high strain rate. Alternatively, this dilemma could be avoided to a large degree through following micro-FTIR measurements on the precracked films under quasi-static stretching conditions.[23]

3.3. Structural Evolution at Crack Tips. Figure 6 shows the IR results obtained from a small region ahead of crack tips during stretching a precracked film of nylon-6/PVDF = 50/50 blends. In the desired wavenumber range two absorption bands belonging to PVDF crystals are observed. The 796 and 841 cm^{-1} band are assigned to the α- and β-form of PVDF component, respectively.[24−26] In the undeformed sample exclusive α-form of PVDF component is presented, consistent with the XRD profiles shown in Figure 3. However, under stretching the content of α-crystals at crack tips gradually decreases, accompanied by the appearance of oriented β-form, i.e., $\alpha \rightarrow \beta$ phase transformation. It means that the dispersed PVDF particles embedded in the nylon-6 matrix can respond to the external force directly and thus incur structural changes due to enough interfacial stress transfer in the nylon-6/PVDF blends with good interfacial adhesion, as the pure PVDF does under deformation.[27−29]

For quantitative analysis of the structural evolution at crack tips, the relative content $F(\beta)$ and dichroic ratio $R(\beta)$ of β-PVDF are deduced using the relations

$$R = A_{\parallel}/A_{\perp} \tag{1}$$

$$A = (A_{\parallel} + 2A_{\perp})/3 \tag{2}$$

$$F(\beta) = \frac{A_{841}}{A_{796} + A_{841}} \tag{3}$$

where $A_{\parallel}$ and $A_{\perp}$ are the parallel and perpendicular absorbance of aforementioned two bands, respectively. Note that the relative absorption coefficient of the 796 to 841 cm^{-1} band is taken as an arbitrary unit, and this treatment has little influence on the tendency of structural evolution during fracture.

In combination with the simultaneous images recorded during fracture process, it is indicated that stress-induced $\alpha \rightarrow \beta$ phase transformation occurs once crack initiation sets in and becomes almost complete before crack propagation (see Figure 6b). Meanwhile, the newly formed β-fibers of PVDF component in the blends become highly elongated at crack tips transverse to the crack propagation direction, as observed by a scanning X-ray scattering study on the structural evolution at crack tips of pure PVDF counterpart.[30] The above results strongly suggest that the plastic deformation and fibrillation of dispersed PVDF particles, as an important energy dissipation process, does take place in the nylon-6/PVDF blends during fracture, consistent with the morphological observations shown in Figure 5. More importantly, the stretching and thinning of the β-fibers at crack tips proceeds via $\alpha \rightarrow \beta$ phase transformation that is also contributed to the energy abosorption,[30] which gives a deep insight into the fracture mechanism over the morphological observations.

4. Conclusion

Incorporation of the dispersed PVDF particles can toughen nylon-6 with high plastic resistance, as the soft rubber particles do. However, the underlying toughening mechanism in the nylon-6/PVDF blends is totally different from that prevailed in the rubber modified polymers, based on morphological observations and in particular the structural evolution at crack tips by micro-FTIR measurements. The $\alpha \rightarrow \beta$ phase transformation and fibrillation of the β-PVDF within the dispersed PVDF particles, as the significant energy dissipation processes, are the toughness enhancing mechanism for the nylon-6/PVDF blends with good interfacial adhesion.

Acknowledgment. The financial support of this work was provided by the National Natural Science Foundation of China (No. 20704006 and 50973017), the Natural Science Foundation of Jiangxi, China (No. 0650009*), and the Project of Jiangxi Provincial Department of Education (No. GJJ08295).

References and Notes

(1) Argon, A. S.; Cohen, R. E. *Polymer* **2003**, *44*, 6013–6032.
(2) Muratoglu, O. K.; Argon, A. S.; Cohen, R. E.; Weinberg, M. *Polymer* **1995**, *36*, 921–930.
(3) Burgisi, G.; Paternoster, M.; Peduto, N.; Saracenos, A. *J. Appl. Polym. Sci.* **1997**, *66*, 777–787.
(4) Huang, J. J.; Paul, D. R. *Polymer* **2006**, *47*, 3505–3519.
(5) Bhattacharyya, A. R.; Ghosh, A. K.; Misra, A.; Eichhorn, K. J. *Polymer* **2005**, *46*, 1661–1674.
(6) Wu, S. *J. Appl. Polym. Sci.* **1988**, *35*, 549–561.

(7) Tzika, P. A.; Boyce, M. C.; Parks, D. M. *J. Mech. Phys. Solids* **2000**, *48*, 1893–1929.
(8) Corté, L.; Leibler, L. *Macromolecules* **2007**, *40*, 5606–5611.
(9) Lazzeri, A.; Bucknall, C. B. *J. Mater. Sci.* **1993**, *28*, 6799–6808.
(10) Wilbrink, M. W. L.; Argon, A. S.; Cohen, R. E.; Weinberg, M. *Polymer* **2001**, *42*, 10155–10180.
(11) He, C.; Liu, T.; Tjiu, W. C.; Sue, H. J.; Yee, A. F. *Macromolecules* **2008**, *41*, 193–202.
(12) Angola, J. C.; Fujita, Y.; Sakai, T.; Inoue, T. *J. Polym. Sci., Part B: Polym. Phys.* **1988**, *26*, 807–816.
(13) Charoensirisomboon, P.; Chiba, T.; Torikai, K.; Saito, H.; Ougizawa, T.; Inoue, T.; Weber, M. *Polymer* **1999**, *40*, 6965–6975.
(14) Kurauchi, T.; Ohta, T. *J. Mater. Sci.* **1984**, *19*, 1699–1709.
(15) Liu, Z. H.; Maréchal, Ph.; Jérôme, R. *Polymer* **1998**, *39*, 1779–1785.
(16) Kim, K. J.; Cho, H. W.; Yoon, K. J. *Eur. Polym. J.* **2003**, *39*, 1249–1265.
(17) Taylor, G. I. *Proc. R. Soc. London A* **1932**, *138*, 41–48.
(18) Wildes, G.; Keskkula, H.; Paul, D. R. *Polymer* **1999**, *40*, 5609–5621.
(19) Nojima, S.; Toei, M.; Hara, S.; Tanimoto, S.; Sasaki, S. *Polymer* **2002**, *43*, 4087–4090.
(20) Loo, Y.; Register, R.; Ryan, A. J.; Dee, G. T. *Macromolecules* **2001**, *34*, 8968–8977.
(21) Tol, R. T.; Mathot, V. B. F.; Groeninckx, G. *Polymer* **2005**, *46*, 369–382.
(22) Ke, Z.; Shi, D.; Yin, J.; Li, R. K. Y.; Mai, Y. W. *Macromolecules* **2008**, *41*, 7264–7267.
(23) Xu, W.; Lv, R.; Na, B.; Tian, N.; Li, Z.; Fu, Q. *J. Phys. Chem. B* **2009**, *113*, 9664–9668.
(24) Salimi, A.; Yousefi, A. A. *Polym. Test.* **2003**, *22*, 699–704.
(25) Lanceros-Méndez, S.; Mano, J. F.; Costa, A. M.; Schmidt, V. H. *J. Macromol. Sci., Phys.* **2001**, *B40*, 517–527.
(26) Yee, W. A.; Nguyen, A. C.; Lee, P. S.; Kotaki, M.; Liu, Y.; Tan, B. T.; Mhaisalkar, S.; Lu, X. *Polymer* **2008**, *49*, 4196–4203.
(27) Sajkiewicz, P.; Wasiak, A.; Goclowski, Z. *Eur. Polym. J.* **1999**, *35*, 423–429.
(28) Quatravaux, T.; Elkoun, S.; G'Sell, C.; Cangemi, L.; Meimon, Y. *J. Polym. Sci., Part B: Polym. Phys.* **2002**, *40*, 2516–2522.
(29) Castagnet, S.; Girault, S.; Gacougnolle, J. L.; Dang, P. *Polymer* **2000**, *41*, 7523–7530.
(30) Maier, G. A.; Wallner, G.; Lang, R. W.; Fratzl, P. *Macromolecules* **2005**, *38*, 6099–6105.